ASSOCIATIVE NEURAL NETWORK MODEL FOR THE GENERATION OF TEMPORAL PATTERNS

Theory and Application to Central Pattern Generators

D. KLEINFELD* AND H. SOMPOLINSKY‡

*Molecular Biophysics Research Department, AT&T Bell Laboratories, Murray Hill, New Jersey 07974; ‡Institute for Theoretical Physics, University of California, Santa Barbara, California 93106; and Racah Institute of Physics, Hebrew University, Jerusalem, Israel 91904

ABSTRACT Cyclic patterns of motor neuron activity are involved in the production of many rhythmic movements, such as walking, swimming, and scratching. These movements are controlled by neural circuits referred to as central pattern generators (CPGs). Some of these circuits function in the absence of both internal pacemakers and external feedback. We describe an associative neural network model whose dynamic behavior is similar to that of CPGs. The theory predicts the strength of all possible connections between pairs of neurons on the basis of the outputs of the CPG. It also allows the mean operating levels of the neurons to be deduced from the measured synaptic strengths between the pairs of neurons. We apply our theory to the CPG controlling escape swimming in the mollusk *Tritonia diomedea*. The basic rhythmic behavior is shown to be consistent with a simplified model that approximates neurons as threshold units and slow synaptic responses as elementary time delays. The model we describe may have relevance to other fixed action behaviors, as well as to the learning, recall, and recognition of temporally ordered information.

INTRODUCTION

The collective properties of highly interconnected networks of model neurons have been the focus of much theoretical analysis. Recent work on this topic involves networks whose dynamics is governed by a cooperative relaxation process (1–5). Starting from an initial state, these networks will relax to one of a select number of stable states. Network models of this form have been used for associative memory (1) and for solving certain optimization problems (6–8). The final, stable states represent the retrieved information or the optimized configuration.

Despite some very suggestive analogies between the network models and biological computational processes, their application in biology is unclear. The difficulty in relating the models to experimental observations reflects, in part, the difficulty in identifying a cooperative relaxational process in large, complex nervous systems. Similarities between associative memory networks and central nervous functions, such as place learning in the hippocampus (9), olfaction (10–12), and visual processing (13) have been proposed. Yet the models remain untested at the level of neurophysiology.

Here we study an associative network model whose collective outputs consist of temporally coherent patterns of linear or cyclic sequences of states (14, 15). This model and its extensions may have a variety of implications for the learning and recall of temporally ordered information. Our objective here is to draw a connection between the properties of the model and biological nervous systems that produce fixed patterns of neural outputs. In particular, we focus on a class of biological systems known as central pattern generators (CPGs).

CPGs control the muscles involved in executing well defined rhythmic behaviors, such as breathing, chewing, walking, swimming, and scratching. Some networks forming CPGs are anatomically well localized and may contain small numbers of neurons. Their output consists of coherent, oscillatory patterns. These features make CPGs strong candidates for studying the relation between output properties of a biological network and its underlying circuitry.

A number of basic principles about CPGs have emerged from studies on a wide variety of rhythmic behaviors (16–21): (a) A rhythmic neural output can occur in the absence of sensory feedback from the muscles and structures controlled by the CPG, and in the absence of control by higher neural centers. These features are clearly demonstrated with spinal preparations (22), i.e., isolated segments of spinal cord. The output activity of the motor neurons in these preparations is similar to the rhythmic firing pattern observed in the intact animal. (b) Some CPGs function without a pacemaker cell, i.e., a single neuron whose firing rate determines the output period of the network. This implies that the rhythmic output is a collective property of the network. Examples include the CPG that controls swimming in the mollusk *Tritonia*

diomedea (23-25) and possibly the CPGs that control flight in the locust (26, 27) and swimming in the leech (28, 29). (*c*) The same set of motor neurons can be involved in a variety of rhythmic behaviors in an animal. This suggests that a CPG may be capable of producing multiple patterns of rhythmic outputs. Further, animals can rapidly switch between rhythmic behaviors and may blend different rhythms together (30).

The model we present may serve as a framework for understanding some biological systems that produce rhythmic output. The network consists of highly interconnected model neurons whose essential feature is a nonlinear relation between their inputs and their output, or mean rate of firing. The form of the output patterns are encoded in the strength of the synaptic connections between pairs of neurons. Thus, our model may be relevant to biological systems in which the strength and time-course of the synaptic connections play the dominant role in the generation of the rhythmic output. The model does not apply to CPGs in which cellular properties are dominant.

Previous theoretical approaches toward understanding CPGs have focused primarily on the mechanism of recurrent cyclic inhibition (31-33). This mechanism forms the basis of networks that function as ring oscillators (34). Alternate theoretical approaches have been described (35-38).

We compare the predictions of our model with Getting's detailed measurements on the CPG controlling the swim rhythm in *Tritonia* (23-25, 39). This CPG contains a small number of neurons and produces a single rhythmic output pattern. Yet the comparison will serve to highlight many features of the model and to assess its applicability to biological systems.

THE MODEL

The present model[1] is an extension of Hopfield's model of associative memory (1, 2). We consider a network that contains N interconnected model neurons. The state of the network is specified by the output activity of all of its neurons. It is represented by $V(t) = \{V_i(t)\}_{i-1}^N$. The output of each neuron, $V_i(t)$, varies between zero (quiescent) and unity (maximum firing rate).

A pattern is defined as a temporal sequence of output states. These states, a subset of all possible output states, are referred to as the embedded states. For example, a pattern of length ℓ consists of the sequence

$$V^1 \rightarrow V^2 \rightarrow V^3 \rightarrow \cdots \rightarrow V^{\ell-1} \rightarrow V^\ell,$$

where each state $V^\mu = \{V_i^\mu\}_{i-1}^N$ is an embedded state. For the case of a cyclic sequence, of relevance for modeling CPGs, $V^1 = V^\ell$. The networks can produce multiple patterns; we define $V^{\mu\nu}$ as the μth embedded state in the νth pattern.

---

[1]The notation in this work differs from that of previous work on this topic, (14,15).

We consider patterns in which the output activity of the model neurons alternatives between a relatively low firing rate and a relatively high rate. The precise form of this activity depends upon the detailed characteristics of the neurons. We therefore assume for simplicity that the output of each neuron alternates between a quiescence and its maximum firing rate. Each component $V_i^{\mu\nu}$ of the embedded states is thus given by either 0 or +1. This assumption allows us to focus on properties of the networks that result specifically from the form of the connections between neurons.

Synaptic Connections and their Response Time

The desired output patterns are encoded in the form of the synaptic connections between the model neurons. We define the synaptic connection between the jth presynaptic neuron and the ith postsynaptic neuron as T_{ij}. A central feature of the present model is that each connection T_{ij} is functionally separated into two components, denoted T_{ij}^S and T_{ij}^L. The two components are hypothesized to have different characteristic response times. The synaptic connections T_{ij}^S act on the shorter of the two times, τ_S. This time determines the time-scale in which the network settles in each of the embedded states. The synaptic connections denoted T_{ij}^L act on the longer time τ_L ($\tau_L \gg \tau_S$). This time sets the time-scale for the onset of the transitions between consecutive states in the pattern. Thus the duration of an individual state in a pattern will be $\sim\tau_L$, while the transitions between states occurs on the faster time-scale of τ_S.

The role of the connection strengths T_{ij}^S is to stabilize the network in an embedded state, until a transition to the next state occurs. This is achieved by defining the T_{ij}^S in terms of a formal version of the Hebb (40) learning rule, i.e.,

$$T_{ij}^S = \frac{J_0}{N} \sum_{\nu-1}^k \sum_{\mu-1}^\ell (2V_i^{\mu\nu} - 1)(2V_j^{\mu\nu} - 1) \quad i \neq j, \quad (1)$$

where k is the total number of patterns, $\ell = \ell(\nu)$ is the length of the νth pattern, $T_{ii}^S = 0$ and $J_0 > 0$. The prefactor J_0/N sets the scale for the magnitude of the average strength of an individual synapse. The variable $(2V_i^{\mu\nu} - 1)$ has a value of either -1 (quiescent) or $+1$ (maximally firing) so that inhibitory as well as excitatory synapses are formed.

The connection strengths T_{ij}^L induce transitions from the μth embedded state to the $(\mu + 1)$-th state. To achieve this, we define

$$T_{ij}^L = \lambda \frac{J_0}{N} \sum_{\nu-1}^k \sum_{\mu-1}^{\ell-1} (2V_i^{\mu+1,\nu} - 1)(2V_j^{\mu\nu} - 1) \quad i \neq j, \quad (2)$$

where λ is a positive scaling parameter for the transition strength and $T_{ii}^L = 0$. For the case of cyclic patterns, $V^{\ell,\nu} = V^{1,\nu}$. Note that the T_{ij}^L synapses, which depend on the consecutive output activity of the neurons, are asymmetric

$(T_{ij}^L \neq T_{ji}^L)$, while the T_{ij}^S synapses, which depend only on the activity within the individual states, are symmetric.

The rule for forming the T_{ij}^L synapses (Eq. 2) encodes transitions between consecutive pairs of embedded states. This allows the network to generate either linear sequences, cyclic sequences, or sequences down a tree structure. Several different patterns, as well as isolated, stable states, can be embedded in the same network. Patterns that involve ambiguous transitions, such as when two patterns share the same state, cannot be reliably produced by the present network. Such patterns can, however, be incorporated by forming synapses that encode transitions between distant states along the pattern (41–43).

The rules defined by Eqs. 1 and 2 for forming the synaptic components are applicable only when the overlaps between the embedded states are small, i.e.,

$$\frac{1}{N} \sum_{j=1}^{N} (2V_j^{\mu,\nu} - 1)(2V_j^{\mu',\nu'} - 1) \simeq 0 \text{ for } (\mu, \nu) \simeq (\mu', \nu') \quad (3)$$

and when, on average, half of the neurons are active in each of the embedded states. Rules that are appropriate for embedding overlapping states in associative networks have been described (44–51).

The integrated synaptic input to each neuron is assumed to be a linear summation of the outputs of the pre-synaptic neurons. The total synaptic input to the ith neuron via the fast components of its synapses, $h_i^S(t)$, is

$$h_i^S(t) = \sum_{j=1}^{N} T_{ij}^S V_j(t). \quad (4)$$

The total synaptic input via the slow components, $h_i^L(t)$, corresponds to a weighted average over the histories of the neural activities, with a characteristic averaging time of τ_L. It is given by

$$h_i^L(t) = \sum_{j=1}^{N} T_{ij}^L \overline{V_j(t)}, \quad (5)$$

where $\overline{V_j(t)}$ is the time-averaged output of the neuron,

$$\overline{V_i(t)} = \int_0^\infty V_i(t - t')w(t') \, dt'. \quad (6)$$

The synaptic response function $w(t)$ for the slow, T_{ij}^L, components is a non-negative function that is normalized to unity and characterized by a mean time-constant τ_L. An example of the time-course of a postsynaptic response to a short presynaptic stimulus is illustrated in Fig. 1 A.

Network Dynamics

Before we define the detailed dynamics of the network, we present a qualitative description in terms of the time dependence of the neural inputs. For simplicity of notation we consider a network that produces a single pattern. Immediately after a transition from the $(\mu - 1)$-th embedded state to the μth state, the output of the network is $V(t) = V^\mu$ and the time-averaged output is $\overline{V(t)} \simeq V^{\mu-1}$.
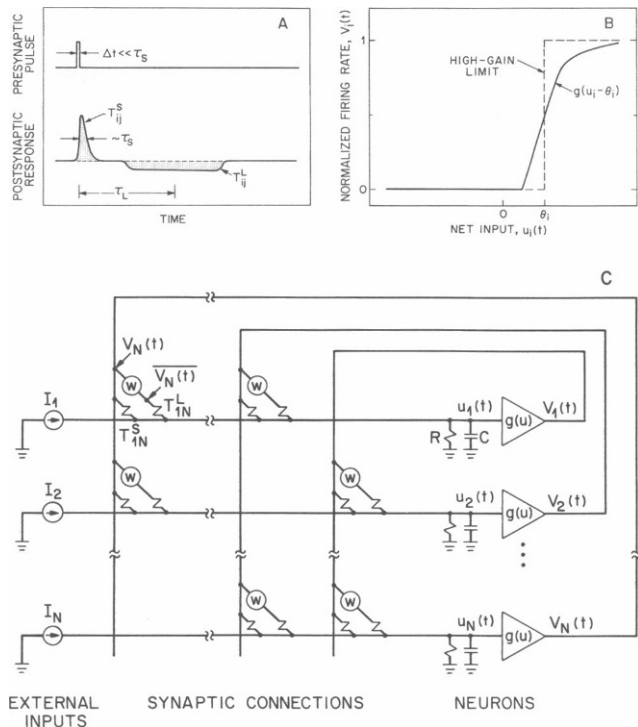

FIGURE 1 Schematic representation of the model network and its components. (A) The time dependent properties of the synaptic connection from the jth to the ith neuron. We illustrate the postsynaptic response observed after a short pulse ($\Delta t \ll \tau_S$) of activity in the presynaptic neuron. The area (*shaded*) under the fast synaptic response for a pulsed input is equal to T_{ij}^S (Eq. 1); in this example we take T_{ij}^S to be excitatory. The area (*shaded*) under the slow synaptic response for a pulsed input is equal to T_{ij}^L (Eq. 2); in this example T_{ij}^L is inhibitory. The ratio of these two areas, averaged over all pairs of synapses, equals the transition strength λ (Eqs. 2 and 3). The time-course of the slow synaptic response corresponds to the response function $w(t)$ (Eq. 5); it has a characteristic time-constant of τ_L. (B) Illustration of a saturating gain function for a neuron. This function relates the output, or firing frequency of a neuron, $V_i(t)$, to the value of its net input, $u_i(t)$, and its mean operating level, θ_i (Eq. 8). The output of a neuron is most sensitive to changes in its inputs when $u_i(t) \simeq \theta_i$. (C) The equivalent circuit describing the model network (Eq. 6). Neurons ($\triangleright$) are represented by saturating amplifiers, as in part B, with a charging time of $RC \leq \tau_S$, where R represents the net input resistance of the neuron and C represents the input capacitance. Synaptic connections between each pair of neurons are represented by conductances ($-\Lambda\Lambda\Lambda-$) proportional to T_{ij}^S or T_{ij}^L, their dynamic properties are illustrated in part A.

The inputs via the fast synaptic components are

$$h_i^S(t) = \sum_{j=1}^{N} T_{ij}^S V_j^\mu \simeq \frac{J_0}{2} (2V_i^\mu - 1), \quad (7)$$

where we used Eqs. 1 and 4 and assumed that the overlap between the V^μ's are small. The synaptic input $h_i^S(t)$ is negative, i.e., inhibitory, if $V_i^\mu = 0$ (quiescent) and is positive, i.e., excitatory, if $V_i^\mu = 1$ (maximally firing). The inputs via the slow synaptic components are (Eqs. 2, 5, and 6)

$$h_i^L(t) = \sum_{j=1}^{N} T_{ij}^L V_j^{\mu-1} \simeq \lambda \frac{J_0}{2} (2V_i^\mu - 1). \quad (8)$$

Thus both $h^S(t)$ and $h^L(t)$ tend to stabilize the network in its current state. With increasing time, $\overline{V(t)}$ gradually shifts away from $V^{\mu-1}$ and toward the current state V^μ. This shift generates an increasingly large component of $h^L(t)$ that is conjugate to $V^{\mu+1}$. After the network has remained in the state V^μ for an interval $\sim\tau_L$, the fast, stabilizing inputs remain unchanged (Eq. 7), but the slow synaptic inputs have evolved to

$$h_i^L(t) - \sum_{j=1}^{N} T_{ij}^L V_j^{\mu-1} \simeq \lambda \frac{J_0}{2} (2V_i^{\mu+1} - 1). \qquad (9)$$

The new values of $h_i^L(t)$ tend to drive the network toward the state $V^{\mu+1}$. For $\lambda \gtrsim 1$ the network makes a rapid transition to the $(\mu + 1)$-th embedded state.

Biological networks, either intrinsically or as a result of damage or disease, may contain only a fraction of all possible synaptic connections. The performance of our network model is only marginally affected when up to half of the fast synaptic components (T_{ij}^S) and the majority of the slow synaptic components (T_{ij}^L) are eliminated at random. The value of the transition strength λ is bounded by

$$\lambda \gtrsim \frac{\text{fraction of } T_{ij}^S \text{ components present}}{\text{fraction of } T_{ij}^L \text{ components present}}. \qquad (10)$$

The detailed dynamic evolution of the network is described by the equations

$$\tau_S \frac{du_i(t)}{dt} + u_i(t) = h_i^S(t) + h_i^L(t) + I_i$$

$$= \sum_{j=1}^{N} [T_{ij}^S V_j(t) + T_{ij}^L \overline{V_j(t)}] + I_i, \qquad (11)$$

where $u_i(t)$ is the net input to the ith neuron and I_i represents an external input. The equivalent electrical circuit described by these equations is shown schematically in Fig. 1 C.

The output of a model neuron, $V_i(t)$, is related to its net input, $u_i(t)$, by a nonlinear gain function

$$V_i(t) = g[u_i(t) - \theta_i], \qquad (12)$$

where we assume that the gain function is approximately sigmoid in sharp. The parameter θ_i is defined as the mean operating level of the neuron[2]; see Fig. 1 B. Note that the dynamic features of the model do not depend on the details of the gain function.[3]

In order that the patterns embedded in the T_{ij}^S and the T_{ij}^L synapses emerge as stable outputs of the network, it is desirable that the output of each neuron is maximally sensitive to changes in its input. This implies that the difference between the mean operating level of a neuron and the net input to that neuron, averaged over all its possible values, must be small. This difference is denoted by $\Delta\theta_i$, where

$$\Delta\theta_i = \theta_i - [u_i(t)]_{avg}$$

$$= \theta_i - \frac{1}{2} \sum_{j=1}^{N} (T_{ij}^S + T_{ij}^L) - I_i(t) \simeq 0. \qquad (13)$$

More precise, we assume that $\Delta\theta_i$ is small compared with the typical value of the total synaptic input that is present while the network is producing a pattern, i.e., $|\Delta\theta_i| \ll J_0$. If $|\Delta\theta_i|$ is comparable with the value of J_0, the stability of the embedded states, and the patterned output, may depend on the precise values of the θ_i's. A similar condition holds for other associative networks (1, 52, 53). Note that Eq. 13 applies only when the embedded states have approximately equal number of active and quiescent neurons and when the gain function of the neurons is approximately sigmoidal.

In the present model the time spent by the network in each embedded state is constant. This time is $t_0 \sim \tau_L$, while the time spent making the transition between two states is $\sim\tau_S$. Thus the period of a cyclic pattern comprised of ℓ states will be $\simeq \ell \cdot t_0$. The time t_0 diverges at $\lambda = \lambda_{critical} \simeq 1$ and monotonically decreases as λ increases above $\lambda_{critical}$.[4] The precise value of t_0 depends on the value of λ, on the detailed form of the synaptic response function, $w(t)$, and on the length of the pattern. An analytical expression that relates these quantities can be derived for network that produces either long patterns or binary oscillations (next section). Details are given elsewhere (14, 81).

Example

We simulated a network consisting of 100 neurons with nine randomly selected embedded states to illustrate how a network can produce multiple, stable output patterns. These states were arranged as a single isolated state, a cyclic pattern among five states, and a cyclic pattern among three states.

---

[2]This definition is more precise than the usual description in the literature on associative neural network models, in which θ_i is equated with the threshold level of a neuron. The later designation, however, is in discord with the neurobiological definition of the threshold level as the minimum input required to elicit a non-zero firing rate. The two definitions are equal only for neurons operating as two-state threshold devices.

[3]More generally, we require that the post-synaptic response of a neuron is a saturating, nonlinear function of its inputs. This can occur even if the firing frequency of the pre-synaptic neuron is a linear function of its input current.

---

[4]The appearance of periodic output in our model is similar to a saddle node bifurcation in the theory of dynamical systems (54). In this bifurcation a stable state, or several stable states, become unstable as a control parameter is varied beyond a critical value (e.g., $\lambda = \lambda_{critical}$ in our case). The system exhibits a periodic motion, characterized by a small frequency but a large amplitude, in which it spends relatively long periods of time near the pervious stable states and makes rapid transitions between these states. In contrast, many weakly nonlinear systems exhibit limit cycles via a normal Hopf bifurcation (54). In this case a periodic motion, with a small amplitude and, typically, high frequencies, forms around the destabilized state.

Fig. 2 A depicts the output pattern from 8 of the 100 neurons. The output is presented in the form of a spike pattern; the individual spikes were generated by a stochastic process in which the output $V_i(t)$ represented the probability that the ith neuron fired in an interval τ_S. This stochastic process may represent rapid fluctuations in cellular or synaptic parameters that control the precise timing of the spike generation. The details of the temporal relation between the synaptic inputs and the output for a particular ($i = 8$) neuron are illustrated in Fig. 2 B; the remainder of the neurons exhibited a similar pattern.

Biphasic Oscillations

A particularly simple pattern is one that oscillates between an embedded state $V^\mu = \{V_i^\mu\}_{i=1}^N$ and its antiphase, $(1 - V^\mu)$, in which the quiescent neurons are now firing and vice versa. Multiple patterns of this form can be embedded in our network. The resulting synaptic strengths are (Eqs. 1 and 2)

$$T_{ij}^S = \frac{J_0}{N} \sum_{\mu=1}^k (2V_i^\mu - 1)(2V_j^\mu - 1), \quad i \neq j \qquad (14)$$

and

$$T_{ij}^L = \lambda \frac{J_0}{N} \sum_{\mu=1}^k [2(1 - V_i^\mu) - 1](2V_j^\mu - 1)$$

$$= -\lambda T_{ij}^S \quad i \neq j, \qquad (15)$$

where k is the number of patterns and $T_{ii}^S = T_{ii}^L = 0$.

Although the synaptic components T_{ij}^L are, in general, asymmetric (i.e., $T_{ji}^L \neq T_{ij}^L$) they are symmetric for the special case of biphasic oscillations (cf. Eqs. 2 and 15). The relation $T_{ij}^L = -\lambda T_{ij}^S$ implies that the connections correspond to either to short-term reciprocal inhibition followed by delayed excitation, or to short-term reciprocal excitation followed by delayed inhibition. Note that the symme-
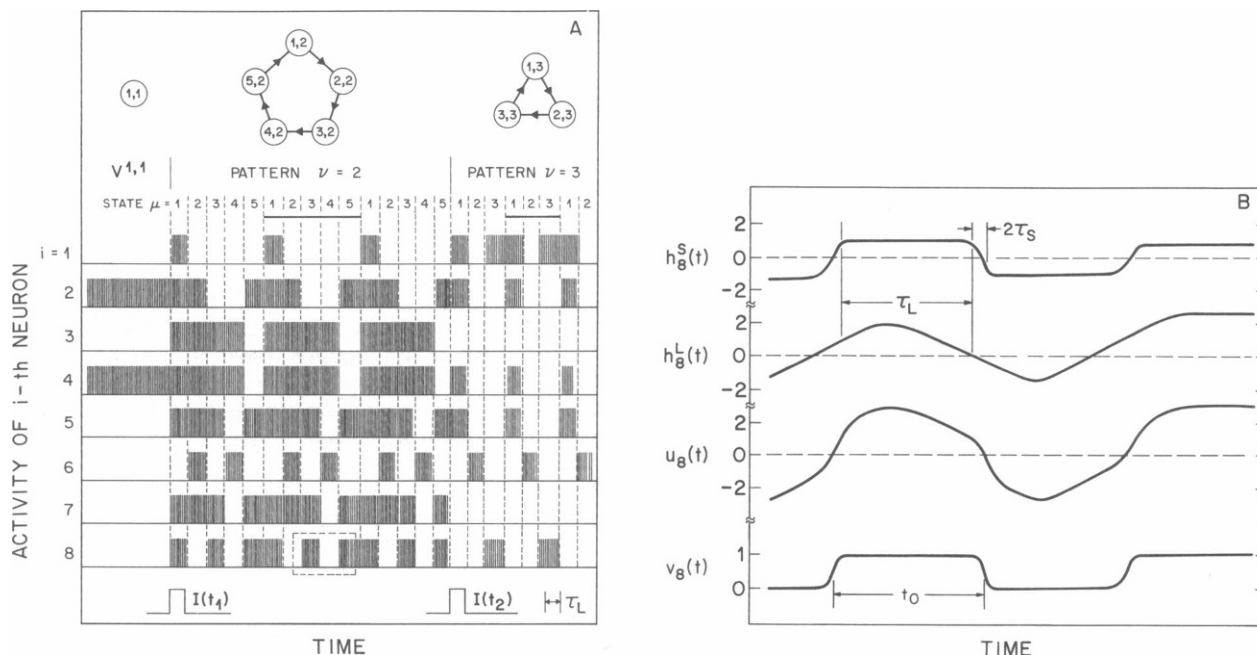

FIGURE 2 Simulation of a network containing 100 neurons with nine embedded states. These states were arranged as a single isolated state, a cyclic pattern among five states, and a cyclic pattern among three states. In this simulation the output of each neuron is either quiescent or firing near its maximum rate. This feature of the output behavior results from the saturation characteristics of the neuron gain function. Other choices for a gain function can lead to stable output patterns in which the firing rate of the neurons does not saturate. (A) The firing pattern calculated from the outputs $V_i(t)$ of 8 of the 100 neurons in the network; the remainder of the neurons showed a similar firing pattern. The network was initially in the isolated, stable state $V^{1,1}$. At time t_1 an external input, $I(t_1)$, was applied for a time τ_L. This input drove the network into state $V^{2,1}$ and thus initiated the ($\nu = 2$)-th pattern. At the later time t_2 a second transient input, $I(t_2)$, was applied to drive the network into the state $V^{1,3}$ and initiate the ($\nu = 3$)-th pattern. The heavy lines at the top of the figure correspond to the output period of each pattern. (B) Details of the dynamic behavior of the ($i = 8$)-th neuron for the period of time delineated by the box in part A. Shown are the inputs from the fast synaptic components, $h_8^S(t)$, the inputs from the slow synaptic components, $h_8^L(t)$, the net synaptic input, $u_8(t)$, and the output of the neuron, $V_8(t)$. The dynamic equations for the network (Eqs. 4 and 8) were approximated using finite difference techniques. The firing rate of the neurons was taken to be described by a sigmoid gain function, i.e., $V_i(t) = 1/2 (1 + \tanh [G \cdot (u_i(t) - \theta_i)])$, where θ_i given by Eq. 8 with $\Delta\theta_i = 0$ and G is the gain constant. In this simulation we used $G^{-1} = J_0/4$ and chose a delayed, uniform-averaging function for the slow synaptic response, i.e., $w(t) = 1/\tau_L$ for $1/2\tau_L < t < 3/2\tau_L$ and $w(t) = 0$ otherwise, with $\tau_L = 20\tau_S$. The slow response function corresponds approximately to that shown in Fig. 1 A. The connection strengths were formed according to Eqs. 1 and 2 using randomly selected embedded states. The transition strength was taken as $\lambda = 2$. We interpreted the values for the neuronal outputs, $V_i(t)$, as the probability that the ith neuron fired in the interval τ_S. These probabilites were used to construct the firing patterns for each neuron.

try in both the T^S_{ij} and the T^L_{ij} components may be broken, e.g., by eliminating synaptic connections, without strongly affecting the output behavior of the network.

Self-Coupling Terms

Our model does not include interactions that feed the output of a neuron back onto itself, i.e., the diagonal elements T^S_{ii} and T^L_{ii} of the synaptic matrices are taken as zero. However, one may need to consider nonzero values for these self-coupling terms when applying our model to a specific biological system. This is particularly relevant when a single neuron in the model represents a group of interacting biological neurons.

When the self-coupling terms are small in magnitude relative to the average total synaptic input from other neurons, i.e., $|T^S_{ii}|$ and $|T^L_{ii}|$ are considerably smaller than J_0 and λJ_0, respectively, they do not disrupt the overall stability of the pattern. Excitatory self-coupling terms will tend to stabilize the embedded states of the network and thus may increase the period of the output pattern. Inhibitory self-coupling terms tend to destabilize the embedded states and thus may decrease the period.

The pattern of output activity may change substantially when the magnitude of the self-coupling terms equals or exceeds the magnitude of the average total synaptic input, i.e., $|T^S_{ii}| \gtrsim J_0$ and $|T^L_{ii}| \gtrsim \lambda J_0$. Under these conditions the dynamics of the network is dominated by the time dependence of the individual neurons, rather than by collective effects.

CENTRAL PATTERN GENERATOR IN *TRITONIA*

We now focus on drawing a connection between our model and detailed measurements on the central pattern generator controlling the swim rhythm in the mollusk *Tritonia diomedea* (23–25, 55, 56). This CPG consists of four neural groups, denoted by *VSI-A*, *VSI-B*, *C2*, and *DSI*. The observed output pattern consists of bursting output from *VSI-A* and *VSI-B* neurons alternating with bursts from the *C2* and *DSI* neurons; Fig. 3 *A*. The output activity lasts for 2–20 cycles.

Of primary importance is Getting's observation that some of the synaptic connections have components that act on different time-scales (23, 25). For example, the synaptic input from *C2* to *DSI* shows a rapid excitatory response followed by a much slower inhibitory response; Fig. 3 *B*. The observed form of the synaptic response in *Tritonia* suggests that there is an analogy between the mechanism for oscillations in our theory and the biological mechanism for oscillations in this CPG.

The thrust of our analysis is to determine if the pattern generated by the CPG in *Tritonia* can be explained by the mechanism we propose for generating patterns. It is important to emphasize that we are not attempting to reproduce the details of the output behavior of *Tritonia*. For this, one
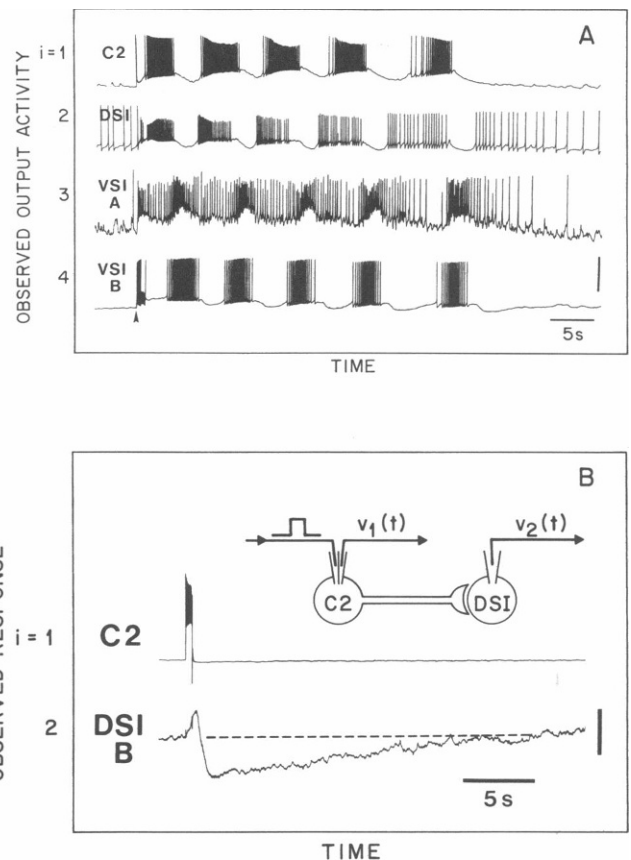

FIGURE 3 The observed behavior of the CPG controlling the escape swim response in *Tritonia*. (*A*) The output activity simultaneously measured from a C2, *DSI*, *VSI-A* and *VSI-B* neuron in an isolated brain preparation from *Tritonia*. These neurons comprise the CPG that controls the escape swim sequence. Their output corresponds to $V_1(t)$, $V_2(t)$, $V_3(t)$, and $V_4(t)$, respectively, in the analysis presented in the text. Vertical bar: 50 mV for C2, *DSI* and *VSI-B* and 25 mV for *VSI-A*. Adapted from Getting (25) with permission. (*B*) An example of the synaptic interaction between two neurons in the CPG in *Tritonia*. Shown is the presynaptic activity measured in the *C2* neuron, $v_1(t)$, and the postsynaptic response measured in a *DSI* neuron, $v_2(t)$, as the result of a short pulse of current injected into *C2*. The measurement was performed under conditions which insured that only monosynaptic connections contributed to the observation. The area under the initial, positive going response corresponds roughly to T^S_{21}; that under the slowly decaying response corresponds to T^L_{21}. The time dependence of the slow decay corresponds to the time dependence of $w(t)$. Vertical bar: 40 mV for *C2* and 2 mV for *DSI*. Adapted from Getting (23) with permission.

would necessarily include the detailed biophysical properties of the neurons and their synaptic connections, as has been discussed for this (24, 57) and other (58) CPGs. For instance, we will not consider the mechanisms for the observed gradual turning off of the output pattern of the CPG.

Synaptic Connections

The observed output sequence is approximated by an oscillation between a state V^+ and its antiphase $V^- \equiv$

$(1 - V^+)$, where

$$V^+ = \begin{pmatrix} \text{activity of } C2 \\ DSI \\ VSI\text{-}A \\ VSI\text{-}B \end{pmatrix} = \begin{pmatrix} +1 \\ +1 \\ 0 \\ 0 \end{pmatrix} \text{ and } V^- = \begin{pmatrix} 0 \\ 0 \\ +1 \\ +1 \end{pmatrix}. \quad (16)$$

These states are used as the stable embedded states in our model. By considering only these two states, we ignore the detailed phase relations during the short transition periods and the phase changes that occur during the gradual turning off of the CPG.

The short-term connection strengths, T_{ij}^S, and the long-term connection strengths, T_{ij}^L, deduced from the stable outputs V^+ and V^- (Eqs. 1, 2, and 16) are shown in Table I. Note that these matrices of synaptic strength contain all possible connections that can be present between pairs of neurons.

How do the predicted synaptic strengths compare with the observed values? The strength of a synaptic connection is proportional to the integral, with respect to time, of the conductance changes induced in the postsynaptic neuron by a short ($t < \tau_S$) pulse of activity in the presynaptic neuron. These integrals can be estimated from intracellular measurements of the potentials induced in the postsynaptic neuron by a short ($t \le \tau_S$) burst of action potentials in the presynaptic neuron under conditions that insure that only monosynaptic pathways contribute to the observed response. In practice, however, the measured postsynaptic response may be effected by a variety of cell membrane properties and by details of the experimental conditions. It may therefore be difficult to accurately estimate the synaptic strengths from available experimental data.

We made a crude classification of the observed synaptic strengths in *Tritonia* based on the pairwise measurements of Getting (23, 25) and on Getting's detailed analysis (57) of the time dependence of the synaptic response. The observed response was classified as either a fast component, T_{ij}^S, or a slow component, T_{ij}^L, according to the time-scale of the decay of the observed synaptic response. Synaptic components that decayed on a time-scale <1 s were designated as fast whereas synaptic components that decayed on a time-scale substantially >1 s were designated as slow.

In our simple analysis, we have considered primarily the sign of the measured post-synaptic response. Thus detailed variations between the values of the individual T_{ij}^S connection strengths and between the T_{ij}^L connection strengths were neglected. For example, the synaptic connection from $C2$ to DSI(Fig. 3 B) was parameterized by the values $T_{2l}^S = +J_0/4$ and $T_{2l}^L = -\lambda J_0/4$. Nevertheless we have not included synaptic components whose strengths are considerably weaker than the rest. The complete set of connection strengths T_{ij}^S and T_{ij}^L are summarized in Table I; a more detailed discussion of the assignments is given later. These synaptic strengths were used to construct the equivalent circuit shown in Fig. 4 A.

The determination of the value of the transition strength, λ, involves a considerable degree of uncertainty. This uncertainty reflects, in part, the difficulty in separating the fast and slow components that contribute to the measured synaptic response. We have considered values of λ in the range $\lambda = 5\text{--}10$ in our simulations. A large value for λ appears to be consistent with the magnitude of the slow versus the fast response observed in some of the synapses, e.g., Fig. 3 B.

The signs of the experimentally observed synaptic

TABLE I
SYNAPTIC CONNECTION STRENGTHS FOR *TRITONIA*

	Fast synaptic components, T_{ij}^S	Slow synaptic components, T_{ij}^L
Theory	$\dfrac{J_0}{4} \begin{pmatrix} 0 & +1 & -1 & -1 \\ +1 & 0 & -1 & -1 \\ -1 & -1 & 0 & +1 \\ -1 & -1 & +1 & 0 \end{pmatrix}$	$\begin{matrix} j = 1 & 2 & 3 & 4 \end{matrix}$ $\lambda\dfrac{J_0}{4} \begin{pmatrix} 0 & -1 & +1 & +1 \\ -1 & 0 & +1 & +1 \\ +1 & +1 & 0 & -1 \\ +1 & +1 & -1 & 0 \end{pmatrix} \begin{matrix} i=1 \\ 2 \\ 3 \\ 4 \end{matrix}$
Observed	$\dfrac{J_0}{4} \begin{pmatrix} 0 & +1 & \bullet & -1 \\ +1 & 0 & -1 & -1 \\ -1 & -1 & 0 & +1 \\ \bullet & -1 & \bullet & 0 \end{pmatrix}$	$\begin{matrix} C & D & VA & VB & pre/post \end{matrix}$ $\lambda\dfrac{J_0}{4} \begin{pmatrix} 0 & \bullet & \bullet & \bullet \\ -1 & 0 & \bullet & \bullet \\ +1 & +1 & 0 & \bullet \\ +1 & \bullet & \bullet & 0 \end{pmatrix} \begin{matrix} C \\ D \\ VA \\ VB \end{matrix}$

The synaptic connection strengths for *Tritonia*. The theoretical values were found using Eqs. 1, 2, and 10. The observed values were abstracted from the data of Getting (23,25); filled circles indicate connections that are not present in *Tritonia*.
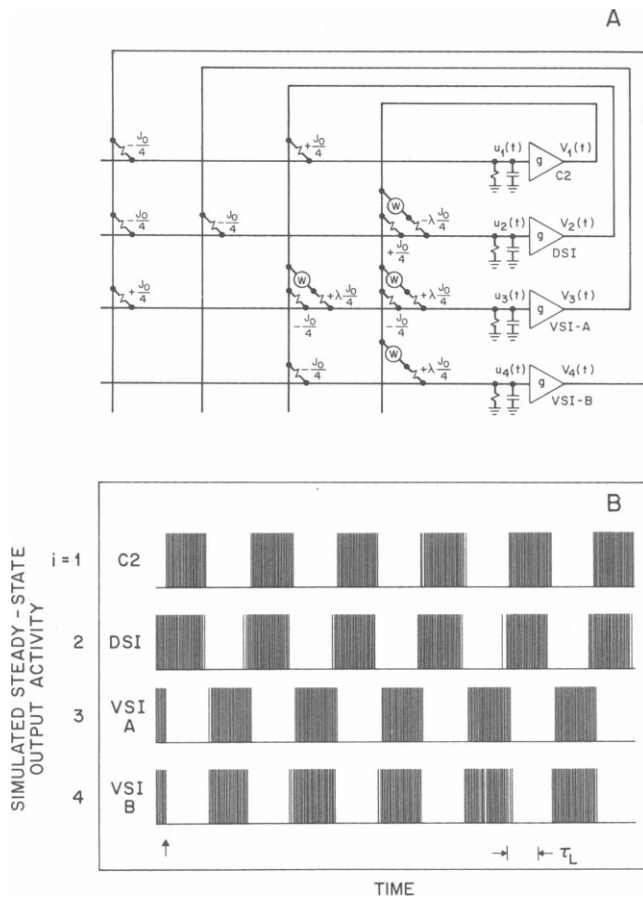
FIGURE 4 The neural network model applied to the CPG in *Tritonia*. (*A*) Schematic representation of the equivalent circuit for the network model; symbols as in Fig. 1. The synaptic strengths contained in the circuit correspond to the observed connections T_{ij}^S and T_{ij}^L (Table I). (*B*) Simulated output activity from the network model in part *A*. The arrows indicates the start of the simulated output from the intial states $V(t < 0) = \overline{V(t < 0)} = (0111)^T$. The dynamic equations for the network were simulated with $G^{-1} = J_0/10$ in the sigmoid gain function defined in the caption for Fig. 2. The slow synaptic response was chose to approximate the response observed in *Tritonia* (Fig. 3 *B*), i.e., $w(t) = 1/\tau_L e^{-t/\tau_L}$ for $0 < t < \infty$ and $w(t) = 0$ otherwise, with $\tau_L = 5\tau_S$. The transition strength was taken as $\lambda = 10$. The period of the simulated output is $2t_0 = 2.5\tau_L$ for this value of λ. The form and timing of the simulated, steady-state output is consistent with the rhythmic behavior observed in *Tritonia* (*cf.* Fig. 3 A).

strengths match those of the theoretically predicted strengths (Table I). Three of the possible twelve synaptic connections show both a short-term and a long-term response. Connections $(i, j) = 3, 1$ and $(i, j) = (3, 2)$ both show short-term inhibition followed by a long-term excitation, while connection $(i, j) = (2, 1)$ shows short-term excitation followed by long-term inhibition. The form of these connections illustrates how the sign of the net synaptic input to a neuron can change over time.

Network Dynamics

We now examine whether our network model, using the synaptic strengths observed for *Tritonia* (Table I), indeed

gives rise to a rhythmic output. We begin with a simplified analysis that accents the role of the synaptic connections in generating stable oscillations. For this analysis we use neurons that are operating in the high-gain limit (Fig. 1 *B*), i.e., $V_i(t + \tau_s) = stp[h_i^S(t) + h_i^L(t) - \theta_i]$, where $stp[x] = +1$ for $x > 1$ and $stp[x] = 0$ otherwise and we take $\Delta\theta_i = 0$ (Eq. [13]). We also employ a delta function delay for the slow synaptic response function, i.e., $w(t) = \delta(t - \tau_L)$.

Immediately after the network has stabilized in the embedded state V^+, the output of the ith neuron is $V_i(t) = V_i^+$, but the delayed output is $\overline{V_i(t)} = V_i(t - \tau_L) = V_i^-$. The output of the ith neuron after the next update, using the matrices containing the observed connection strengths (Table I), is

$$V_i(t + \tau_S) = stp\left\{\sum_{j=1}^{4} [T_{ij}^S (2V_j^+ - 1) + T_{ij}^L (2V_j^- - 1)]\right\}$$

$$= \begin{pmatrix} +1 \\ +1 \\ 0 \\ 0 \end{pmatrix} = V_i^+ \quad (17)$$

for $\lambda > 0$. Thus the output of the network is stable on the time-scale of τ_S. After the network has remained in the state V^+ for a time τ_L, the delayed output changes to $\overline{V(t + \tau_L)} = V(t) = V^+$. The output of the ith neuron after the next update is

$$V_i(t + \tau_L + \tau_S) = stp\left\{\sum_{j=1}^{4} [T_{ij}^S (2V_j^+ - 1) + T_{ij}^L (2V_j^+ - 1)]\right\}$$

$$= \begin{pmatrix} +1 \\ 0 \\ +1 \\ +1 \end{pmatrix} \quad (18)$$

For $\lambda > 3$. The network is now in a mixed, unstable state. Using this new value for the current state in the update procedure gives

$$V_i(t + \tau_L + 2\tau_S) = stp\left\{\sum_{j=1}^{4} [T_{ij}^S (2V_j(t + \tau_L + \tau_S) - 1)\right.$$

$$\left. + T_{ij}^L (2V_j^+ - 1)]\right\} = \begin{pmatrix} 0 \\ 0 \\ +1 \\ +1 \end{pmatrix} = V_i^-. \quad (19)$$

The network has now completed a transition from the state V^+ to the state V^-. It will remain in this state for a time $t_0 \simeq \tau_L$, after which the cycle will repeat itself. The output of the network will oscillate only if the transition strength is $\lambda < 3$ (Eq. 18).

The simplified analysis presented above suggests that the mechanism for rhythmic output proposed by the model may be applicable to the CPG in *Tritonia*. To further ascertain the correspondence between the model and the observed properties of this CPG, we studied the dynamics of the model network using parameters appropriate for *Tritonia*. Eqs. 11–13 were simulated using the observed connection strengths (Fig. 4 *A*), analog neurons (Fig. 1 *B*) and a synaptic response function $w(t)$ that decays exponentially over time; this function approximates the response observed in *Tritonia* (57). Stable oscillations of the form described by the previous simplified analysis (Eqs. 17–19) were observed. The output activity for the transition strength $\lambda = 10$ is shown in Fig. 4 *B*.

The period of the rhythmic output, $2t_0$, depends on the values of τ_L, λ, and on the form of $w(t)$. We estimated the value of t_0, deduced from the theory by both analytical and numerical methods using $\tau_S \leq 0.5$ s, the observed range of $\tau_L = 2$ s to 5 s (57), $\lambda = 5$ to 10 and $w(t)$ as described above. The calculated period was $2 < 2t_0/\tau_L < 4$ for the range of parameters $5 \leq \lambda \leq 10$ and $5 \leq \tau_L/\tau_S \leq 10$; this implies $2t_0 = 4$s to 20s. The lower estimate, corresponding to $\lambda \approx 10$, is in accord with the experimental value (25) of $2t_0 = 6$s to 10s (Fig. 3 *A*).

Neuron Operating Levels

We now consider the issue of the mean operating level of each neuron, θ_i. In order for the network to produce a stable, rhythmic pattern, the firing rate of each neuron must be sensitive to changes in the value of its input. The values of θ_i that optimize this sensitivity are given by Eq. 13. For the connections in *Tritonia*, this relation becomes

$$\theta_i \simeq I_i + \frac{1}{2}\sum_{j-1}^{4}(T_{ij}^S + T_{ij}^L) - I_i + \frac{J_0}{8}\begin{pmatrix} 0 \\ -1-\lambda \\ -1+2\lambda \\ -1+\lambda \end{pmatrix} \quad (20)$$

with $\lambda > 3$. Consider the *DSI* neuron first ($i = 2$). Eq. 20 implies either that this neuron should be in a tonically excited state when it is functionally isolated from its synaptic inputs ($\theta_2 < 0$), or that this neuron requires an external excitatory input for the CPG to be active ($I_2 > 0$). A combination of both of these features is observed in vivo (24, 39). The *DSI* neurons fire tonically, although at a considerably reduced rate, in isolation (24). Activation of the CPG in *Tritonia* requires an effective excitatory input to the *DSI* neurons (39). After this input is removed, the output from the CPG gradually looses its temporal coherence and the CPG becomes inactive. We next consider the *VSI* neurons. In the absence of synaptic inputs and external inputs, the output of *VSI-B* is expected to be quiescent ($\theta_4 > 0$). This result is in agreement with observation (25).

The problematic neuron is *VSI-A*. This neuron is not known to receive an external input while the CPG is producing oscillatory output. Thus, according to Eq. 20, *VSI-A* should have a positive operating level. In practice, *VSI-A* exhibits a weak tonic output when it is functionally isolated (24). Violation of Eq. 20 suggests that the oscillations in the output of *VSI-A* will be less robust than that of the other neurons. This conclusion is consistent with the observed outputs, i.e., the relative change in the firing rate of *VSI-A* during the oscillations is smaller than that of the other neurons (Fig. 4 *B*).

Assumptions in Assigning the Synaptic Strengths

Several assumptions were made in assigning the observed connection strengths. The connection from *DSI* to *C2* exhibits short-term excitation followed by a much weaker long-term excitation. We ignored the weak long-term effect; thus $T_{12}^S = +J_0/4$ and $T_{12}^L = 0$. Similarly we have ignored the weak, extremely slow inhibition ($\tau \sim 15$ s) that appeared in some measurements of the synaptic coupling from *VSI-B* to the *DSI*; thus $T_{24}^S = -J_0/4$ and $T_{24}^L = 0$. This component does not appear to play a significant role in controlling the dynamics of the network on the time-scale, $t_0 < 5$ s, of the rhythmic output (P. A. Getting—private communication).

The observed synaptic connection from the *DSI* to *VSI-A* exhibits two short-term responses as well as a long-term response. Short-term inhibition is preceded by a relatively shorter period of excitation, with the pair followed by long-term excitation. We ignored the initial, relatively short excitation and assigned $T_{32}^S = -J_0/4$ and $T_{32}^L = +\lambda J_0/4$. A different choice for the sign of T_{32}^S does not significantly affect the output pattern of the network.

The synaptic coupling between *VSI-A* and *VSI-B* could not be measured under conditions that suppressed possible indirect interactions, i.e., poly-synaptic pathways, between these neurons (25). Intracellular excitation of *VSI-B* caused *VSI-A* to weakly fire; we assigned $T_{34}^S = +J_0/4$ and $T_{34}^L = 0$. Excitation of *VSI-A* caused a slow depolarization in *VSI-B*, but did not cause it to fire. We chose $T_{43}^S = T_{43}^L = 0$, but one cannot rule out the possibility $T_{43}^S = 0$ and $T_{43}^L > 0$. An analysis of the network dynamics showed that stable oscillations persist if T_{43}^L is excitatory, so long as it is weaker (by $\sim 25\%$ or more) than the other slow synaptic components.

Interactions Among the *DSI* Neurons

There are three ipsilateral *DSI* neurons, connected to each other via excitatory connections (23). Noting that these cells fire in synchrony with each other when the CPG is active (23) and that functional removal of some of these cells does not effect the basic rhythmic output (39), we grouped all three *DSI* as a single neuron. The role of the

DSI as separate neurons pertains to the turning on and turning off of the cyclic response (39), a topic we do not consider in detail.

The fast excitatory interaction among the *DSI* neurons can be incorporated by including a nonzero self-coupling term, T_{22}^S, in the model. An analysis of the network dynamics shows that inclusion of this term has a relatively small effect on the output of the network. For example, the period increased by only 10% when the self-coupling strength was set equal to the typical strength of the other synaptic inputs, i.e., $T_{22}^S = +J_0/4$. Some of the *DSI* connections exhibit a slow excitatory component. This can be modeled by taking a nonzero value for T_{22}^L. The magnitude of this term must be assigned with care. There is only one (dominant) slow synaptic input to the *DSI* from the other neurons, i.e., $T_{21}^L = -\lambda J_0/4$, and thus the rhythmic output will be disrupted for $T_{22}^L \gtrsim +\lambda J_0/4$. However, an analysis of the network dynamics for *Tritonia* shows that the rhythmic output is not appreciably effected if $T_{22}^L \lesssim +0.5 \lambda J_0/4$. This constraint on T_{22}^L is consistent with the observed couplings strengths (23, 57).

DISCUSSION

The present model for generating output patterns has several attractive structural and functional features. It describes pattern generation in arbitrarily large, highly interconnected networks. The model does not necessarily rely on specific organization of the connections, (e.g., a ring-like organization [34] or a Petri net [59]). The synaptic connections are not symmetric and the network can contain both excitatory and inhibitory synapses. It can also operate with only inhibitory connections. The distributed nature of the network and the inherent feedback between neurons endow the network with a high robustness.

Our model does not use pacemaking cells or a system clock to generate patterns. Rather, the sequential output results from the interplay between fast synaptic components, which stabilize the embedded states, and slow synaptic components, which trigger the transitions. The detailed form of the slow synaptic response is not critical. The network will function properly so long as most of the slow components have roughly the same time-constant.

The network can produce multiple patterns of different lengths and topologies. Neither the embedded states nor the patterns need to have any specific structure. In fact, the model works optimally with patterns of random, uncorrelated states. An individual pattern can be accessed in an associative manner, such as by an input that only partially resembles one of the embedded states in the pattern. Well defined mechanisms exist for modulating the output period of a pattern and for switching between patterns. Lastly, the model employs a simple relation between the output patterns and the synaptic connections.

Analysis of the CPG in Tritonia

We used our associative network model to analyze the CPG controlling the swim rhythm in the mollusc *Tritonia*. The basic rhythmic output could be accounted for by a simplified analysis that employed threshold units as neurons and that replaced the response function of the slow synapses by a simple time-delay. This analysis served to emphasize the role of the connections between neurons in determining the collective output of this CPG.

This sign and time course of the observed synaptic strengths were in accord with the values predicted by the formalized Hebb (40) learning rules (Eqs. 1 and 2). This suggests the utility of such rules for predicting the strength of the underlying synaptic connections from the observed output states.

Our analysis demonstrates that, within the framework of our model, even a small network can function with the elimination of many of its theoretically possible connections. Many more fast synapses than slow synapses are present in *Tritonia*. The fast synaptic components stabilize the output states, and thus relatively few of these synapses can be eliminated (i.e., 25% of all possible T_{ij}^S's are eliminated; see Table I). Partial elimination of the slow synaptic components can be offset by an increase in the transition strength, λ. This compensation may occur in *Tritonia*.

Our analysis also showed how the required balance between the mean operating level of each neuron and the value of its external inputs and the strength of its synaptic connections can be simply estimated. We argued that the mean operating level of the *VSI-A* neuron in *Tritonia* is set too low. This result explained the relatively weak changes in the firing activity of *VSI-A* during periods of otherwise active output by the CPG (Fig. 3 *A*). Our result futher suggests that the activity of *VSI-A* will alternate more sharply between bursting and silence if its operating value is raised, e.g., by the injection of a small hyperpolarizing current.

Multiphasic Synapses and Synaptic Delays

A variety of biophysical and biochemical mechanisms allow synapses to act on more than a single time-scale (60). Chemically mediated synapses can show both fast and slow responses, as well as a combination of the two. For example, the synaptic connections in *Tritonia* act on time-scales that differ by up to a factor of thirty (23). Some of the chemically-mediated synapses present in the network controlling the flight rhythm in the locust exhibit a delayed excitatory response (27). Chemically-mediated synapses in the stomatogastric ganglion of the lobster exhibit both prompt and delayed inhibitory repsonses (61). Electrotonic connections provide a potential mechanism for the presence of both slow and fast synapses in a network. The high resistance of these couplings between

neurons in the CPG controlling feeding in the snail *Helisoma* cause their response time to be an order of magnitude slower than other synapses in the network (62). The converse situation occurs in the circuit controlling feeding in the mollusc *Navanax*, where the electrotonic couplings act rapidly compared with the chemically-mediated synapses (63). Synaptic delays can also result from the delays inherent in active propagation along a relatively long process and when the synaptic connections T_{ij}^L between pairs of neurons are mediated by interneurons.

Neurons may contain cellular as well as synaptic delays. Cellular delays can affect the response time of a neuron to many or all of its synaptic inputs. When the response time of the cellular delay is short compared with the slow synaptic response time, τ_L, the separation of the time-scales between τ_S and τ_L is maintained and the output properties of the network model are unaffected. On the other hand, some well characterized cellular delays can be considered in terms of an effective synaptic delay. For example, the outward potassium current I_A (64, 65) is partially responsible for the delayed response of the *VSI-B* neuron in *Tritonia* (25, 57). This current has the effect of allowing only slow excitatory inputs into *VSI-B*, but does not affect the time-scale of the inhibitory connections.

Lastly, our model is capable of producing rhythmic output in large networks that contain only monophasic connections. In this case, a synapse has either a fast response time or a slow response time, but not both. The strength of each synapse is chosen according to the formalized Hebb rules (Eqs. 1 and 2), but the minimum value of the transition strength, λ, depends on the relative number of fast versus slow connections (Eq. 10). This suggests that our model may be appropriate for analyzing CPGs that do not contain multiphasic synapses.

Modulation of the Output

The output activity of many CPGs can be initiated and modulated by external inputs from command neurons (66, 67) or from circulating neurohormones (68–70). Large changes in the period of the output can occur if the external inputs or neurohormones affect either the time-constant of the slow synaptic response, τ_L, or the transition strength, λ. For example, a neuromodulator that selectively augments the strength of the slow synaptic components, or diminishes that of the fast components, will shorten the period of the output. It will be interesting to see if neurophysiological correlates for these and related predictions are found.

It should be emphasized that we have considered so far only networks with parameters, e.g., synaptic strengths, neuron operating levels, and external inputs, that do not change in time. Biologically these parameters undergo slow changes, such as increases (facilitation) or decreases (fatigue) in the values of the synaptic strengths. This slow change may modulate the overall behavior of the network. For example, a gradual change in the mean operating levels or an external input will dephase the output pattern of a CPG. This will eventually terminate the oscillatory output, similar to the effect of the slowly decreasing tonic input to the CPG in *Tritonia* (Fig. 3 *A*) (39, 71).

Learning and Plasticity

One of the central features of the model is the simple relationship between the output patterns and the connections, i.e., the formalized Hebb learning rules (Eqs. 1 and 2). These rules allow new patterns to be embedded in the network by modifying the synapses both incrementally in time and locally in space; the change to each synapse depends only on the activities of the postsynaptic and presynaptic neurons during the learning of the new pattern. Local updating of the synapses makes the present model particularly suitable for large, complex systems that are continuously updated as patterns are modified or added. This feature also pertains to some other network models of sequence generation (41, 72–75).

We introduced the relation between the sequential form of the T_{ij}^L synapses (Eq. 2) and their slow dynamic response (Eqs. 5 and 6) as an *ad-hoc* assumption. These two features may, in fact, be closely related to each other. If one considers the evolution of the synaptic strengths in terms of a dynamic learning mechanism, the different final forms of the T_{ij}^S and the T_{ij}^L synaptic components may be the result of the different time-scale of their dynamic response. For example, the T_{ij}^S components can relate two experiences that are separated by the characteristic response time of the slow components, while the T_{ij}^S components can only aid in recalling the presence of either experience. It would be interesting to test this idea in a biologically plausible model of learning. Finally, we note two other potential applications of the model. One involves the relation between learning rules that depend on the history of neuronal activity and the temporal associations inherent in classical conditioning (76–78). A second involves the recognition of sequences of sensory input (15, 42, 79, 80).

REFERENCES

1. Hopfield, J. J. 1982. Neural networks and physical systems with emergent collective computational abilities. *Proc. Natl. Acad. Sci. USA.* 79:2554–2558.

2. Hopfield, J. J. 1984. Neurons with graded response have collective computational properties like those of two-state neurons. *Proc. Natl. Acad. Sci. USA.* 81:3088–3092.

3. Peretto, P. 1984. Collective properties of neural networks: a statistical approach. *Biol Cybern.* 50:51–62.

4. Amit, D. J., H. Gutfreund, and H. Sompolinsky. 1985. Spin-glass models of neural networks. *Phys. Rev. A.* 32:1007–1018.

5. Amit, D. J., H. Gutfreund, and H. Sompolinsky. 1985. Storing infinite numbers of patterns in a spin-glass model of neural networks. *Phys. Rev. Lett.* 55:1530–1533.

6. Hopfield, J. J., and D. W. Tank. 1985. "Neural" computation of decisions in optimization problems. *Biol. Cybern.* 52:141–152.

7. Jeffrey, W., and R. Rosner. 1986. Optimization algorithms: simulated annealing and neural network processing. *Astrophys. J.* 310:473–481.

8. Hopfield, J. J., and D. W. Tank. 1986. Computing with neural circuits: a model. *Science (Wash. DC).* 233:625–632; 235:1226–1229 (comments).

9. O'Keefe, J. 1983. Spatial memory with and without the hippocampal system. *In* Neurobiology of the Hippocampus. W. Seifert, editor. Academic Press Inc., NY.

10. Gelperin, A., J. J. Hopfield, and D. W. Tank. 1985. *In* Model Neural Networks and Behavior. A. I. Selverston, editor. Plenum Publishing Corp., NY.

11. Haberly, L. B. 1985. Neural circuitry in olfactory cortex: anatomy and functional implications. *Chem. Sens.* 10:219–238.

12. Baird, B. 1986. Nonlinear dynamics of pattern formation and pattern recognition in the rabbit olfactory cortex. *Physica D.* 22:150–175.

13. Koch, C., J. Marroquin, and A. Yuille. 1986. Analog "neural" networks in early vision. *Proc. Natl. Acad. Sci. USA.* 83:4263–4267.

14. Sompolinsky, H., and I. Kanter. 1986. Temporal association in asymmetric neural networks. *Phys. Rev. Lett.* 57:2861–2864.

15. Kleinfeld, D. 1986. Sequential state generation by model neural networks. *Proc. Natl. Acad. Sci. USA.* 83:9469–9473.

16. Delcomyn, F. 1980. Neural basis of rhythmic behavior in animals. *Science (Wash. DC).* 210:492–498.

17. Kristan Jr., W. B. 1980. Generation of rhythmic motor patterns. *In* Information Processing in the Nervous System. H. M. Pinsker and W. D. Willis, Jr., editors. Raven Press, NY.

18. Selverston, A. I. 1980. Are central pattern generators understandable? *Behav. Brain Sci.* 3:535–571.

19. Roberts, A., and B. L. Roberts. 1983. Neural Origin of Rhythmic Movements. Cambridge University Press, Cambridge, UK.

20. Cohen, A. H., S. Rossignol, and S. Grillner. 1988. Neural Control of Rhythmic Movements. John Willey & Sons Inc., New York.

21. Selverston, A. I., and M. Moulins. 1986. The Crustacean Stomatogastric System. Springer-Verlag, New York, Inc., NY.

22. Grillner, S. 1975. Locomotion in vertebrates. Control mechanisms and reflex interaction. *Physiol. Rev.* 55:247–304.

23. Getting, P. A. 1981. Mechanism of pattern generation underlying swimming in *Tritonia.* I. Neuronal network by monosynaptic connections. *J. Neurophysiol.* (Bethesda). 46:65–79.

24. Getting, P. A. 1983. Mechanism of pattern generation underlying swimming in *Tritonia.* II. Network reconstruction. *J. Neurophysiol. (Bethesda)* 49:1017–1035.

25. Getting, P. A. 1983. Mechanism of pattern generation underlying swimming in *Tritonia.* III. Intrinsic and synaptic mechanisms for delayed excitations. *J. Neurophysiol. (Bethesda).* 49:1036–1050.

26. Wilson, D. M. 1961. The central nervous control of flight in a locust. *J. Exp. Biol.* 38:471–490.

27. Robertson, M., and K. G. Pearson. 1985. Neural circuits in the flight system of the locust. *J. Neurophysiol.* (Bethesda). 53:110–128.

28. Stent, G. S., W. B. Kristan Jr., W. O. Friesen, C. A. Ort, M. Poon, and R. L. Calabrese. 1978. Neural generation of the leech swimming movement. *Science (Wash. DC).* 200:1348–1356.

29. Weeks, J. C. 1981. Neuronal basis of leech swimming: separation of swim initiation, pattern generation, and intersegmental coordination by selective lesions. *J. Neurophysiol. (Bethesda).* 45:698–723.

30. Stein, P. S. G., A. W. Camp, G. A. Robertson, and L. I. Mortin. 1986. Blends of rostral and caudal scratch reflex motor patterns elicited by the simultaneous stimulation of to sites in the spinal turtle. *J. Neurosci.* 6:2259–2266.

31. Reiss R. F. 1964. A theory of resonance networks. *In* Neural theory and Modeling. R. F. Reiss, editor. Stanford University Press. Standford, CA.

32. Harmon, L. D. 1964. Neuromines: Action of a reciprocally inhibitory pair. *Science (Wash. DC).* 146:1323–1325.

33. Wilson, D. M., and I. Waldron. 1968. Models for the generation of the motor output pattern in flying locusts. *Proc. IEEE.* 56:1058–1064.

34. Kling, U., and G. Székely. 1968. Simulation of rhythmic activities. I. Function of networks with cyclic inhibitions. *Kybernetik.* 5:89–103.

35. Harth, E., and N. S. Lewis, and T. J. Csermely. 1975. Escape of *Tritonia:* dynamics of neuromuscular control mechanisms. *J. Theor. Biol.* 55:210–228.

36. Glass, L., and R. E. Young. 1979. Structure and dynamics of neural network oscillators. *Brain. Res.* 179:208–218.

37. Kopell, N. 1986. *In* Lecture in Notes Biomathematics 66. H. Othmer, editor. Springer-Verlag, New York, Inc., NY.

38. Thompson, R. S. 1982. A model for basic pattern generating mechanisms in the lobster stomatogastic ganglion. *Biol. Cybern.* 43:71–78.

39. Getting, P. A., and M. S. Dekin. 1985. Mechanism of pattern generation underlying swimming in *Tritonia.* IV. Gating of central pattern generator. *J. Neurophysiol. (Bethesda).* 53:466–480.

40. Hebb, D. O. 1949. The Organization of Behavior: A Neuropsychological Theory. John Wiley & Sons New York.

41. Fukushima, K. 1973. A model of associative memory in the brain. *Kybernetik.* 12:58–63.

42. Tank, D. W., and J. J. Hopfield. 1987. Neural computation by time compression. *Proc. Natl. Acad. Sci. USA.* 84:1896–1900.

43. Keeler, J. D. 1988. Comparison between sparsely distributed memory and Hopfield-type neural network models. *J. Cognitive Sci.* In press.

44. Kohonen, T., and M. Ruohonen. 1973. Representation of associated data by matrix operators. *IEEE Trans. Comput.* 22:701–702.

45. Personnaz, L., I. Guyon, and G. Dreyfus. 1986. Information storage and retrieval in spin-glass like neural networks. *J. Phys. Lett.* 46:359–365.

46. Denker, J. S. 1986. Neural network models of learning and adaptation. *Physica D.* 22:216–232.

47. Kanter, I., and H. Sompolinsky. 1987. Associative recall of memory without errors. *Phys. Rev. A.* 35:380–392.

48. Diederich, S., and M. Opper. 1987. Learning of correlated patterns in spin-glass networks by local learning rules. *Phys. Rev. Lett.* 58:949–952.

49. Amit, D. J., H. Gutfreund, and H. Sompolinsky. 1987. Information storage in neural networks with low levels of activity. *Phys. Rev. A.* 35:2293–2303.

50. E. Gardner. 1988. The space of interactions in neural network models. *J. Phys. A.* 21:257–270.

51. E. Garnder, and B. Derrida. 1988. Optimal storage properties of neural network models. *J. Phys. A.* 21:271–284.

52. Little, W. A. 1974. The existence of persistent states in the brain. *Math. Biosci.* 19:101–120.

53. Bruce, A. D., E. J. Gardner, and D. J. Wallace. 1987. Static and dynamic properties of the Hopfield model. *J. Phys. A.* 20:2909–2934.

54. Guckenheimer, J., and P. Holmes. 1983. Nonlinear oscillations, dynamical systems and bifurcations of vector fields. Springer-Verlag, New York, Inc., NY.

55. Willows, A. D. O. 1967. Behavioral acts elicited by simulation of single, identifiable brain cells. *Science (Wash. DC).* 157:570–574.

56. Willows, A. D. O., and G. Hoyle. 1969. Neural network triggering of fixed action pattern. *Science (Wash. DC).* 166:1549–1551.

57. Getting, P. A. 1988. Reconstruction of small neural networks. *In* Methods in Neuronal Modeling: From Synapses to Networks. C. Koch and I. Segev, editors. MIT Press, Cambridge, MA.

58. Hartline, D. K. 1979. Pattern generation in the lobster (*Panulirus*) stomatogastric ganglion. II. Pyloric network simulation. *Biol. Cybern.* 33:223–236.

59. J. C. Platt. 1985. Sequential threshold circuits. California Institute of Technology Report 5197:TR:85.

60. Kehoe, J., and A. Marty. 1980. Certain slow synaptic responses: their properties and possible underlying mechanisms. *Annu. Rev. Biophys. Bioeng.* 9:437–465.

61. Hartline, D. K., and D. V. Gassie Jr. 1979. Pattern generation in the lobster (*Panulirus*) stomatogastric ganglion. Pyloric neuron kinetics and synaptic interactions. *Biol. Cybern.* 33:209–222.

62. Kaneko, C. R. S., M. Merickel, and S. B. Kater. 1978. Central programmed feeding in *Helisoma:* identification and characteristics of an electrically coupled premotor neuron network. *Brain Res.* 126:1–21.

63. Spray, D. C., M. E. Spira, and M. V. L. Bennett. 1980. Synaptic connections of buccal mechanosensory neurons in the opisthobranch mollusc, *Navanax inermis. Brain Res.* 182:271–286.

64. Neher, E. 1971. Two fast transient current components during voltage clamp on snail neurons. *J. Gen. Physiol.* 58:36–53.

65. oConnor, J. A., and C. F. Stevens. 1971. Voltage clamp studies of a transient outward membrane current in gastropod neural soma. *J. Physiol. (Lond.).* 213:21–30.

66. Kennedy, D., W. H. Evoy, and J. T. Hanawaly. 1966. Release of coordinated activity in crayfish by single central neurons. *Science (Wash. DC).* 154:917–919.

67. Kupfermann, I. and K. R. Weiss. 1978. The command neuron concept. *Behav. Brain Sci.* 1:3–39.

68. Pinsker, H. M., and J. Ayers. 1983. Neuronal Oscillators. *In* The Clinical Neurosciences. W. D. Eillis, editor. Churchill Livingstone Inc., New York.

69. Marder, E., and S. L. Hooper. 1985. Neurotransmitter modulation of the stomatogastric ganglion of decapod crustacean. *In* Model Neural Networks and Behavior. A. I. Selverston, editor. Plenum Publishing Corp., New York.

70. Harris-Warrick, R. M. 1986. Chemical modulation of central pattern generators. *In* Neural Control of Rhythmic Movements. A. H. Cohen, S. Rossignol, and S. Grillner, editors. John Wiley & Sons Inc., New York.

71. Lennard, P. R., P. A. Getting, and R. I. Hume. 1980. Central pattern generator mediating swimming in *Tritonia:* II. Initiation, maintenance, and termination. *J. Neurophysiol. (Bethesda).* 44:165–173.

72. Kohonen, T. 1980. Content-Addressable Memories. Springer-Verlag New York, Inc., NY.

73. Peretto, P., and J. J. Niez. 1986. Collective properties of neural networks. *In* Disordered Systems and Biological Organization. E. Bienenstock, F. Fogelman, and G. Weisbuch, editors. Springer-Verlag, New York, Inc., N.Y.

74. Dehaene, S., J.-P. Changeux, and J.-P. Nadel. 1987. Neural networks that learn temporal sequences by selection. *Proc. Natl. Acad. Sci. USA.* 84:2727–2731.

75. Buhmann, J., and K. Schulten. 1987. Noise-driven temporal association in neural networks. *Europhys. Lett.* 4:1205–1209.

76. Tesauro, G. J. 1986. Simple neural models of classical conditioning. *Biol. Cybern.* 55:187–200.

77. Barto, A. G., and R. S. Sutton, 1982. Simulation of anticipatory responses in classical conditioning by a neuron-like adaptive element. *Behav. Brain. Sci.* 4:221–235.

78. Klopf, A. H. 1987. A drive-reinforcement model of single neuron function: An alternative to the Hebbian neuronal model. *Air Force Wright Aeronautical Laboratories preprint.*

79. Amit, D. J. 1988. Neural networks counting chimes. *Proc. Natl. Acad. Sci. USA.* 85:2141–2145.

80. Gutfreund, H., and M. Mezárd. 1988. Processing of temporal sequences in neural networks. *Phys. Rev. Lett.* 61:235–238.

81. Kleinfeld, D., and H. Sompolinsky. 1988. An associative network model for central pattern generators. *In* Methods in Neuronal Modeling: From Synapses to Networks. C. Koch and I. Segev, editors. MIT Press, Cambridge, MA.